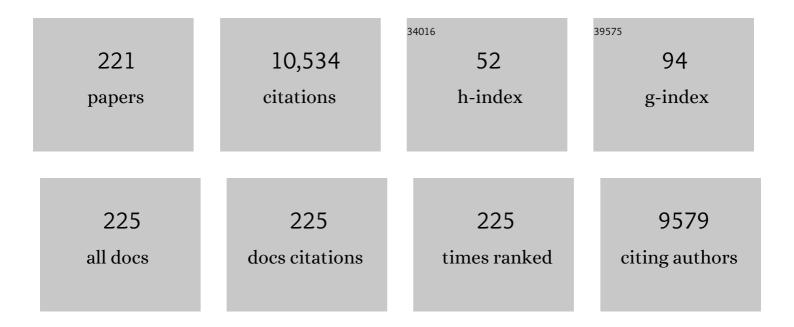
List of Publications by Year in descending order

Source: https://exaly.com/author-pdf/5023999/publications.pdf Version: 2024-02-01



#	Article	IF	CITATIONS
1	Real-Time Spatiotemporal Spectral Unmixing of MODIS Images. IEEE Transactions on Geoscience and Remote Sensing, 2022, 60, 1-16.	2.7	2
2	MACU-Net for Semantic Segmentation of Fine-Resolution Remotely Sensed Images. IEEE Geoscience and Remote Sensing Letters, 2022, 19, 1-5.	1.4	36
3	SSA-SiamNet: Spectral–Spatial-Wise Attention-Based Siamese Network for Hyperspectral Image Change Detection. IEEE Transactions on Geoscience and Remote Sensing, 2022, 60, 1-18.	2.7	30
4	Multiattention Network for Semantic Segmentation of Fine-Resolution Remote Sensing Images. IEEE Transactions on Geoscience and Remote Sensing, 2022, 60, 1-13.	2.7	92
5	Geographically Weighted Spatial Unmixing for Spatiotemporal Fusion. IEEE Transactions on Geoscience and Remote Sensing, 2022, 60, 1-17.	2.7	6
6	A Self-Training Hierarchical Prototype-based Ensemble Framework for Remote Sensing Scene Classification. Information Fusion, 2022, 80, 179-204.	11.7	16
7	Fast and Slow Changes Constrained Spatio-Temporal Subpixel Mapping. IEEE Transactions on Geoscience and Remote Sensing, 2022, 60, 1-16.	2.7	0
8	Semantic Segmentation of Terrestrial Laser Scanning Point Clouds Using Locally Enhanced Image-Based Geometric Representations. IEEE Transactions on Geoscience and Remote Sensing, 2022, 60, 1-15.	2.7	5
9	A taxonomic-based joint species distribution model for presence-only data. Journal of the Royal Society Interface, 2022, 19, 20210681.	1.5	1
10	Spatial sampling, data models, spatial scale and ontologies: Interpreting spatial statistics and machine learning applied to satellite optical remote sensing. Spatial Statistics, 2022, 50, 100646.	0.9	4
11	Unmet need for COVID-19 vaccination coverage in Kenya. Vaccine, 2022, 40, 2011-2019.	1.7	13
12	A deep learning model for incorporating temporal information in haze removal. Remote Sensing of Environment, 2022, 274, 113012.	4.6	12
13	Geoscience-aware deep learning: A new paradigm for remote sensing. Science of Remote Sensing, 2022, 5, 100047.	2.2	17
14	Modeling the efficacy of different anti-angiogenic drugs on treatment of solid tumors using 3D computational modeling and machine learning. Computers in Biology and Medicine, 2022, 146, 105511.	3.9	10
15	A joint distribution framework to improve presenceâ€only species distribution models by exploiting opportunistic surveys. Journal of Biogeography, 2022, 49, 1176-1192.	1.4	3
16	Forecasting of Built-Up Land Expansion in a Desert Urban Environment. Remote Sensing, 2022, 14, 2037.	1.8	15
17	Near real-time surface water extraction from GOES-16 geostationary satellite ABI images by constructing and sharpening the green-like band. Science of Remote Sensing, 2022, 5, 100055.	2.2	1
18	UNetFormer: A UNet-like transformer for efficient semantic segmentation of remote sensing urban scene imagery. ISPRS Journal of Photogrammetry and Remote Sensing, 2022, 190, 196-214.	4.9	206

#	Article	IF	CITATIONS
19	The Forgotten Semantics of Regression Modeling in Geography. Geographical Analysis, 2021, 53, 113-134.	1.9	2
20	Sociodemographic determinants of COVID-19 incidence rates in Oman: Geospatial modelling using multiscale geographically weighted regression (MGWR). Sustainable Cities and Society, 2021, 65, 102627.	5.1	138
21	Spatial–Spectral Radial Basis Function-Based Interpolation for Landsat ETM+ SLC-Off Image Gap Filling. IEEE Transactions on Geoscience and Remote Sensing, 2021, 59, 7901-7917.	2.7	18
22	A Semi-Supervised Deep Rule-Based Approach for Complex Satellite Sensor Image Analysis. IEEE Transactions on Pattern Analysis and Machine Intelligence, 2021, PP, 1-1.	9.7	3
23	Estimating Artificial Impervious Surface Percentage in Asia by Fusing Multi-Temporal MODIS and VIIRS Nighttime Light Data. Remote Sensing, 2021, 13, 212.	1.8	9
24	An Improved Index for Urban Population Distribution Mapping Based on Nighttime Lights (DMSP-OLS) Data: An Experiment in Riyadh Province, Saudi Arabia. Remote Sensing, 2021, 13, 1171.	1.8	19
25	Blocks-removed spatial unmixing for downscaling MODIS images. Remote Sensing of Environment, 2021, 256, 112325.	4.6	33
26	Ensembles of multiple spectral water indices for improving surface water classification. International Journal of Applied Earth Observation and Geoinformation, 2021, 96, 102278.	1.4	3
27	Global land cover trajectories and transitions. Scientific Reports, 2021, 11, 12814.	1.6	29
28	Association between community-based self-reported COVID-19 symptoms and social deprivation explored using symptom tracker apps: a repeated cross-sectional study in Northern Ireland. BMJ Open, 2021, 11, e048333.	0.8	6
29	Spatio-temporal spectral unmixing of time-series images. Remote Sensing of Environment, 2021, 259, 112407.	4.6	44
30	Fine temporal resolution satellite sensors with global coverage: an opportunity for landscape ecologists. Landscape Ecology, 2021, 36, 2199-2213.	1.9	7
31	A Scale Sequence Object-based Convolutional Neural Network (SS-OCNN) for crop classification from fine spatial resolution remotely sensed imagery. International Journal of Digital Earth, 2021, 14, 1528-1546.	1.6	14
32	Explainable artificial intelligence: an analytical review. Wiley Interdisciplinary Reviews: Data Mining and Knowledge Discovery, 2021, 11, e1424.	4.6	198
33	Tracking small-scale tropical forest disturbances: Fusing the Landsat and Sentinel-2 data record. Remote Sensing of Environment, 2021, 261, 112470.	4.6	32
34	The Role of Earth Observation in Achieving Sustainable Agricultural Production in Arid and Semi-Arid Regions of the World. Remote Sensing, 2021, 13, 3382.	1.8	11
35	Filling gaps in Landsat ETM+ÂSLC-off images with Sentinel-2 MSI images. International Journal of Applied Earth Observation and Geoinformation, 2021, 101, 102365.	1.4	16
36	Iterative Deep Learning (IDL) for agricultural landscape classification using fine spatial resolution remotely sensed imagery. International Journal of Applied Earth Observation and Geoinformation, 2021, 102, 102437.	1.4	5

#	Article	IF	CITATIONS
37	Integrating spatio-temporal-spectral information for downscaling Sentinel-3 OLCI images. ISPRS Journal of Photogrammetry and Remote Sensing, 2021, 180, 130-150.	4.9	15
38	Object-Based Area-to-Point Regression Kriging for Pansharpening. IEEE Transactions on Geoscience and Remote Sensing, 2021, 59, 8599-8614.	2.7	13
39	ABCNet: Attentive bilateral contextual network for efficient semantic segmentation of Fine-Resolution remotely sensed imagery. ISPRS Journal of Photogrammetry and Remote Sensing, 2021, 181, 84-98.	4.9	106
40	Automatic Extraction and Labelling of Memorial Objects From 3D Point Clouds. Journal of Computer Applications in Archaeology, 2021, 4, 79-93.	0.8	5
41	Resilience of the Central Indian Forest Ecosystem to Rainfall Variability in the Context of a Changing Climate. Remote Sensing, 2021, 13, 4474.	1.8	7
42	Using Daily Nighttime Lights to Monitor Spatiotemporal Patterns of Human Lifestyle under COVID-19: The Case of Saudi Arabia. Remote Sensing, 2021, 13, 4633.	1.8	11
43	Scale-Aware Neural Network for Semantic Segmentation of Multi-Resolution Remote Sensing Images. Remote Sensing, 2021, 13, 5015.	1.8	11
44	Spatial analysis of G.f.fuscipes abundance in Uganda using Poisson and Zero-Inflated Poisson regression models. PLoS Neglected Tropical Diseases, 2021, 15, e0009820.	1.3	4
45	Collective influence of household and community capitals on agricultural employment as a measure of rural poverty in the Mahanadi Delta, India. Ambio, 2020, 49, 281-298.	2.8	15
46	Evaluating the impact of declining tsetse fly (Glossina pallidipes) habitat in the Zambezi valley of Zimbabwe. Geocarto International, 2020, 35, 1373-1384.	1.7	2
47	A Geostatistical Filter for Remote Sensing Image Enhancement. Mathematical Geosciences, 2020, 52, 317-336.	1.4	3
48	Information Loss-Guided Multi-Resolution Image Fusion. IEEE Transactions on Geoscience and Remote Sensing, 2020, 58, 45-57.	2.7	10
49	Scale Sequence Joint Deep Learning (SS-JDL) for land use and land cover classification. Remote Sensing of Environment, 2020, 237, 111593.	4.6	76
50	Identifying and mapping individual plants in a highly diverse high-elevation ecosystem using UAV imagery and deep learning. ISPRS Journal of Photogrammetry and Remote Sensing, 2020, 169, 280-291.	4.9	54
51	Dynamic susceptibility mapping of slow-moving landslides using PSInSAR. International Journal of Remote Sensing, 2020, 41, 7509-7529.	1.3	12
52	Virtual image pair-based spatio-temporal fusion. Remote Sensing of Environment, 2020, 249, 112009.	4.6	67
53	The effect of the point spread function on downscaling continua. ISPRS Journal of Photogrammetry and Remote Sensing, 2020, 168, 251-267.	4.9	15
54	General solution to reduce the point spread function effect in subpixel mapping. Remote Sensing of Environment, 2020, 251, 112054.	4.6	29

#	Article	IF	CITATIONS
55	Investigating the Influence of Registration Errors on the Patch-Based Spatio-Temporal Fusion Method. IEEE Journal of Selected Topics in Applied Earth Observations and Remote Sensing, 2020, 13, 6291-6307.	2.3	7
56	COVID-19 Outbreak Prediction with Machine Learning. Algorithms, 2020, 13, 249.	1.2	218
57	Biospytial: spatial graph-based computing for ecological Big Data. GigaScience, 2020, 9, .	3.3	5
58	Sub-pixel mapping with point constraints. Remote Sensing of Environment, 2020, 244, 111817.	4.6	22
59	A Special Issue on the Importance of Geostatistics in the Era of Data Science. Mathematical Geosciences, 2020, 52, 311-315.	1.4	8
60	Incorporating spatial association into statistical classifiers: local pattern-based prior tuning. International Journal of Geographical Information Science, 2020, 34, 2077-2114.	2.2	3
61	Two-Phase Object-Based Deep Learning for Multi-Temporal SAR Image Change Detection. Remote Sensing, 2020, 12, 548.	1.8	22
62	Crop classification from full-year fully-polarimetric L-band UAVSAR time-series using the Random Forest algorithm. International Journal of Applied Earth Observation and Geoinformation, 2020, 87, 102032.	1.4	34
63	Quantifying the Effect of Registration Error on Spatio-Temporal Fusion. IEEE Journal of Selected Topics in Applied Earth Observations and Remote Sensing, 2020, 13, 487-503.	2.3	24
64	Principles and methods of scaling geospatial Earth science data. Earth-Science Reviews, 2019, 197, 102897.	4.0	66
65	Agricultural shocks and drivers of livelihood precariousness across Indian rural communities. Landscape and Urban Planning, 2019, 189, 307-319.	3.4	35
66	Three-Fold Urban Expansion in Saudi Arabia from 1992 to 2013 Observed Using Calibrated DMSP-OLS Night-Time Lights Imagery. Remote Sensing, 2019, 11, 2266.	1.8	37
67	A hybrid OSVM-OCNN Method for Crop Classification from Fine Spatial Resolution Remotely Sensed Imagery. Remote Sensing, 2019, 11, 2370.	1.8	14
68	Photoperiod controls vegetation phenology across Africa. Communications Biology, 2019, 2, 391.	2.0	34
69	Identifying the spatio-temporal risk variability of avian influenza A H7N9 in China. Ecological Modelling, 2019, 414, 108807.	1.2	5
70	An Iterative Coarse-to-Fine Sub-Sampling Method for Density Reduction of Terrain Point Clouds. Remote Sensing, 2019, 11, 947.	1.8	9
71	Multisource and Multitemporal Data Fusion in Remote Sensing: A Comprehensive Review of the State of the Art. IEEE Geoscience and Remote Sensing Magazine, 2019, 7, 6-39.	4.9	302
72	Dramatic Loss of Agricultural Land Due to Urban Expansion Threatens Food Security in the Nile Delta, Egypt. Remote Sensing, 2019, 11, 332.	1.8	85

#	Article	IF	CITATIONS
73	Downscaling Gridded DEMs Using the Hopfield Neural Network. IEEE Journal of Selected Topics in Applied Earth Observations and Remote Sensing, 2019, 12, 4426-4437.	2.3	3
74	Joint Deep Learning for land cover and land use classification. Remote Sensing of Environment, 2019, 221, 173-187.	4.6	285
75	Full year crop monitoring and separability assessment with fully-polarimetric L-band UAVSAR: A case study in the Sacramento Valley, California. International Journal of Applied Earth Observation and Geoinformation, 2019, 74, 45-56.	1.4	20
76	A Massively Parallel Deep Rule-Based Ensemble Classifier for Remote Sensing Scenes. IEEE Geoscience and Remote Sensing Letters, 2018, 15, 345-349.	1.4	45
77	Downscaling AMSR-2 Soil Moisture Data With Geographically Weighted Area-to-Area Regression Kriging. IEEE Transactions on Geoscience and Remote Sensing, 2018, 56, 2362-2376.	2.7	36
78	Characterising the land surface phenology of Africa using 500Âm MODIS EVI. Applied Geography, 2018, 90, 187-199.	1.7	38
79	Rice crop phenology mapping at high spatial and temporal resolution using downscaled MODIS time-series. GIScience and Remote Sensing, 2018, 55, 659-677.	2.4	41
80	Enhancing spectral unmixing by considering the point spread function effect. Spatial Statistics, 2018, 28, 271-283.	0.9	8
81	Mapping paddy rice fields by applying machine learning algorithms to multi-temporal Sentinel-1A and Landsat data. International Journal of Remote Sensing, 2018, 39, 1042-1067.	1.3	101
82	Forecasting wheat and barley crop production in arid and semi-arid regions using remotely sensed primary productivity and crop phenology: A case study in Iraq. Science of the Total Environment, 2018, 613-614, 250-262.	3.9	63
83	Remote sensing of mangrove forest phenology and its environmental drivers. Remote Sensing of Environment, 2018, 205, 71-84.	4.6	137
84	Spatio-temporal fusion for daily Sentinel-2 images. Remote Sensing of Environment, 2018, 204, 31-42.	4.6	234
85	A hybrid MLP-CNN classifier for very fine resolution remotely sensed image classification. ISPRS Journal of Photogrammetry and Remote Sensing, 2018, 140, 133-144.	4.9	284
86	National and sub-national variation in patterns of febrile case management in sub-Saharan Africa. Nature Communications, 2018, 9, 4994.	5.8	38
87	Spatial-temporal fraction map fusion with multi-scale remotely sensed images. Remote Sensing of Environment, 2018, 213, 162-181.	4.6	30
88	Largeâ€scale prerain vegetation greenâ€up across Africa. Global Change Biology, 2018, 24, 4054-4068.	4.2	29
89	VPRS-Based Regional Decision Fusion of CNN and MRF Classifications for Very Fine Resolution Remotely Sensed Images. IEEE Transactions on Geoscience and Remote Sensing, 2018, 56, 4507-4521.	2.7	51
90	An object-based convolutional neural network (OCNN) for urban land use classification. Remote Sensing of Environment, 2018, 216, 57-70.	4.6	313

#	Article	IF	CITATIONS
91	Major trends in the land surface phenology (LSP) of Africa, controlling for land-cover change. International Journal of Remote Sensing, 2018, 39, 8060-8075.	1.3	6
92	A new multi-resolution based method for estimating local surface roughness from point clouds. ISPRS Journal of Photogrammetry and Remote Sensing, 2018, 144, 369-378.	4.9	8
93	An agent-based model of tsetse fly response to seasonal climatic drivers: Assessing the impact on sleeping sickness transmission rates. PLoS Neglected Tropical Diseases, 2018, 12, e0006188.	1.3	17
94	Approximate Area-to-Point Regression Kriging for Fast Hyperspectral Image Sharpening. IEEE Journal of Selected Topics in Applied Earth Observations and Remote Sensing, 2017, 10, 286-295.	2.3	8
95	Spectral–Spatial Adaptive Area-to-Point Regression Kriging for MODIS Image Downscaling. IEEE Journal of Selected Topics in Applied Earth Observations and Remote Sensing, 2017, 10, 1883-1896.	2.3	11
96	Asteroid impact effects and their immediate hazards for human populations. Geophysical Research Letters, 2017, 44, 3433-3440.	1.5	41
97	Population vulnerability models for asteroid impact risk assessment. Meteoritics and Planetary Science, 2017, 52, 1082-1102.	0.7	15
98	Enhancing Spatio-Temporal Fusion of MODIS and Landsat Data by Incorporating 250 m MODIS Data. IEEE Journal of Selected Topics in Applied Earth Observations and Remote Sensing, 2017, 10, 4116-4123.	2.3	38
99	Fusion of Landsat 8 OLI and Sentinel-2 MSI Data. IEEE Transactions on Geoscience and Remote Sensing, 2017, 55, 3885-3899.	2.7	121
100	The effect of the point spread function on sub-pixel mapping. Remote Sensing of Environment, 2017, 193, 127-137.	4.6	37
101	Treatment-seeking behaviour in low- and middle-income countries estimated using a Bayesian model. BMC Medical Research Methodology, 2017, 17, 67.	1.4	16
102	Learning-Based Spatial–Temporal Superresolution Mapping of Forest Cover With MODIS Images. IEEE Transactions on Geoscience and Remote Sensing, 2017, 55, 600-614.	2.7	26
103	Mapping the birch and grass pollen seasons in the UK using satellite sensor time-series. Science of the Total Environment, 2017, 578, 586-600.	3.9	45
104	RECENT trends in the land surface phenology of africa observed at a fine spatial scale. , 2017, , .		0
105	Malaria prevalence metrics in low- and middle-income countries: an assessment of precision in nationally-representative surveys. Malaria Journal, 2017, 16, 475.	0.8	11
106	Significance of major international seaports in the distribution of murine typhus in Taiwan. PLoS Neglected Tropical Diseases, 2017, 11, e0005430.	1.3	18
107	Advances in mapping malaria for elimination: fine resolution modelling of Plasmodium falciparum incidence. Scientific Reports, 2016, 6, 29628.	1.6	32
108	Spatio-temporal analysis of malaria vector density from baseline through intervention in a high transmission setting. Parasites and Vectors, 2016, 9, 637.	1.0	15

#	Article	IF	CITATIONS
109	On the influence of impact effect modelling for global asteroid impact risk distribution. Acta Astronautica, 2016, 123, 165-170.	1.7	19
110	Area-to-point regression kriging for pan-sharpening. ISPRS Journal of Photogrammetry and Remote Sensing, 2016, 114, 151-165.	4.9	60
111	<i>Hyalomma</i> ticks on northward migrating birds in southern Spain: Implications for the risk of entry of Crimean-Congo haemorrhagic fever virus to Great Britain. Journal of Vector Ecology, 2016, 41, 128-134.	0.5	25
112	Global impact risk of known asteroids. , 2016, , .		1
113	Modelling the spatial-temporal distribution of tsetse (Glossina pallidipes) as a function of topography and vegetation greenness in the Zambezi Valley of Zimbabwe. Applied Geography, 2016, 76, 198-206.	1.7	6
114	A multiple-point spatially weighted <i>k</i> -NN classifier for remote sensing. International Journal of Remote Sensing, 2016, 37, 4441-4459.	1.3	10
115	Fusion of Sentinel-2 images. Remote Sensing of Environment, 2016, 187, 241-252.	4.6	163
116	Anisotropy Characteristics of Exposed Gravel Beds Revealed in High-Point-Density Airborne Laser Scanning Data. IEEE Geoscience and Remote Sensing Letters, 2016, 13, 1044-1048.	1.4	2
117	Spatiotemporal Subpixel Mapping of Time-Series Images. IEEE Transactions on Geoscience and Remote Sensing, 2016, 54, 5397-5411.	2.7	24
118	A systematic review of vegetation phenology in Africa. Ecological Informatics, 2016, 34, 117-128.	2.3	72
119	Moving interdisciplinary science forward: integrating participatory modelling with mathematical modelling of zoonotic disease in Africa. Infectious Diseases of Poverty, 2016, 5, 17.	1.5	32
120	Novel shape indices for vector landscape pattern analysis. International Journal of Geographical Information Science, 2016, 30, 2442-2461.	2.2	11
121	Extravagance in the commons: Resource exploitation and the frontiers of ecosystem service depletion in the Amazon estuary. Science of the Total Environment, 2016, 550, 6-16.	3.9	17
122	Classification of Vegetation Type in Iraq Using Satellite-Based Phenological Parameters. IEEE Journal of Selected Topics in Applied Earth Observations and Remote Sensing, 2016, 9, 414-424.	2.3	24
123	The global impact distribution of Near-Earth objects. Icarus, 2016, 265, 209-217.	1.1	17
124	The Sero-epidemiology of Coxiella burnetii in Humans and Cattle, Western Kenya: Evidence from a Cross-Sectional Study. PLoS Neglected Tropical Diseases, 2016, 10, e0005032.	1.3	68
125	A Multi-Host Agent-Based Model for a Zoonotic, Vector-Borne Disease. A Case Study on Trypanosomiasis in Eastern Province, Zambia. PLoS Neglected Tropical Diseases, 2016, 10, e0005252.	1.3	7
126	Mapping Soil Health over Large Agriculturally Important Areas. Soil Science Society of America Journal, 2015, 79, 1420-1434.	1.2	39

#	Article	IF	CITATIONS
127	Characterising the Land Surface Phenology of Europe Using Decadal MERIS Data. Remote Sensing, 2015, 7, 9390-9409.	1.8	39
128	Spatiotemporal Variation in Mangrove Chlorophyll Concentration Using Landsat 8. Remote Sensing, 2015, 7, 14530-14558.	1.8	57
129	Spatiotemporal Variation in Surface Urban Heat Island Intensity and Associated Determinants across Major Chinese Cities. Remote Sensing, 2015, 7, 3670-3689.	1.8	101
130	The potential of satellite-observed crop phenology to enhance yield gap assessments in smallholder landscapes. Frontiers in Environmental Science, 2015, 3, .	1.5	35
131	Evaluating the Impact of the Community-Based Health Planning and Services Initiative on Uptake of Skilled Birth Care in Ghana. PLoS ONE, 2015, 10, e0120556.	1.1	42
132	Exploiting Human Resource Requirements to Infer Human Movement Patterns for Use in Modelling Disease Transmission Systems: An Example from Eastern Province, Zambia. PLoS ONE, 2015, 10, e0139505.	1.1	5
133	Spatiotemporal variation in the terrestrial vegetation phenology of Iraq and its relation with elevation. International Journal of Applied Earth Observation and Geoinformation, 2015, 41, 107-117.	1.4	20
134	Sleeping sickness and its relationship with development and biodiversity conservation in the Luangwa Valley, Zambia. Parasites and Vectors, 2015, 8, 224.	1.0	25
135	A Multiple-Mapping Kernel for Hyperspectral Image Classification. IEEE Geoscience and Remote Sensing Letters, 2015, 12, 978-982.	1.4	9
136	Downscaling remotely sensed imagery using area-to-point cokriging and multiple-point geostatistical simulation. ISPRS Journal of Photogrammetry and Remote Sensing, 2015, 101, 174-185.	4.9	35
137	Poverty, health and satellite-derived vegetation indices: their inter-spatial relationship in West Africa. International Health, 2015, 7, 99-106.	0.8	24
138	Downscaling MODIS images with area-to-point regression kriging. Remote Sensing of Environment, 2015, 166, 191-204.	4.6	126
139	Tsetse Fly (G.f. fuscipes) Distribution in the Lake Victoria Basin of Uganda. PLoS Neglected Tropical Diseases, 2015, 9, e0003705.	1.3	26
140	A novel multi-parameter support vector machine for image classification. International Journal of Remote Sensing, 2015, 36, 1890-1906.	1.3	14
141	Fine spatial resolution residential land-use data for small-area population mapping: a case study in Riyadh, Saudi Arabia. International Journal of Remote Sensing, 2015, 36, 4315-4331.	1.3	10
142	Accuracy of Digital Elevation Models Derived From Terrestrial Laser Scanning Data. IEEE Geoscience and Remote Sensing Letters, 2015, 12, 1923-1927.	1.4	23
143	Land Cover Change Detection at Subpixel Resolution With a Hopfield Neural Network. IEEE Journal of Selected Topics in Applied Earth Observations and Remote Sensing, 2015, 8, 1339-1352.	2.3	66
144	Interpreting predictive maps of disease: highlighting the pitfalls of distribution models in epidemiology. Geospatial Health, 2014, 9, 237.	0.3	9

PETER M ATKINSON

#	Article	IF	CITATIONS
145	Climate variability and anthropogenic impacts on a semi-distributed monsoon catchment runoff simulations. , 2014, , .		8
146	An effective approach for gap-filling continental scale remotely sensed time-series. ISPRS Journal of Photogrammetry and Remote Sensing, 2014, 98, 106-118.	4.9	156
147	Sub-pixel mapping of remote sensing images based on radial basis function interpolation. ISPRS Journal of Photogrammetry and Remote Sensing, 2014, 92, 1-15.	4.9	93
148	Remotely sensed trends in the phenology of northern high latitude terrestrial vegetation, controlling for land cover change and vegetation type. Remote Sensing of Environment, 2014, 143, 154-170.	4.6	115
149	Propagation of vertical and horizontal source data errors into a TIN with linear interpolation. International Journal of Geographical Information Science, 2014, 28, 1378-1400.	2.2	14
150	The effect of short ground vegetation on terrestrial laser scans at a local scale. ISPRS Journal of Photogrammetry and Remote Sensing, 2014, 95, 42-52.	4.9	33
151	Modelling the Incidence of Plasmodium vivax and Plasmodium falciparum Malaria in Afghanistan 2006–2009. PLoS ONE, 2014, 9, e102304.	1.1	24
152	Ecological sustainability in rangelands: the contribution of remote sensing. International Journal of Remote Sensing, 2013, 34, 6216-6242.	1.3	39
153	Downscaling in remote sensing. International Journal of Applied Earth Observation and Geoinformation, 2013, 22, 106-114.	1.4	172
154	Decadal length changes in the fluvial planform of the River Ganga: bringing a mega-river to life with Landsat archives. Remote Sensing Letters, 2013, 4, 1-9.	0.6	52
155	Exploring the links between census and environment using remotely sensed satellite sensor imagery. Journal of Land Use Science, 2013, 8, 284-303.	1.0	13
156	Validation of the MODIS reflectance product under UK conditions. International Journal of Remote Sensing, 2013, 34, 7376-7399.	1.3	2
157	Remote sensing of river bathymetry for use in hydraulic model prediction of flood inundation. , 2012, ,		5
158	Inter-comparison of four models for smoothing satellite sensor time-series data to estimate vegetation phenology. Remote Sensing of Environment, 2012, 123, 400-417.	4.6	385
159	Modelling the bulk flow of a bedrockâ€constrained, multiâ€channel reach of the Mekong River, Siphandone, southern Laos. Earth Surface Processes and Landforms, 2012, 37, 533-545.	1.2	9
160	Autologistic modelling of susceptibility to landsliding in the Central Apennines, Italy. Geomorphology, 2011, 130, 55-64.	1.1	84
161	Exploring the impact of climate and land use changes on streamflow trends in a monsoon catchment. International Journal of Climatology, 2011, 31, 815-831.	1.5	78
162	A characterisation of climate variability and trends in hydrological extremes in the Severn Uplands. International Journal of Climatology, 2011, 31, 1634-1652.	1.5	24

PETER M ATKINSON

#	Article	IF	CITATIONS
163	A comparison of gauge and radar precipitation data for simulating an extreme hydrological event in the Severn Uplands, UK. Hydrological Processes, 2011, 25, 795-810.	1.1	38
164	Image fusion by spatially adaptive filtering using downscaling cokriging. ISPRS Journal of Photogrammetry and Remote Sensing, 2011, 66, 337-346.	4.9	53
165	Super-resolution mapping using Hopfield Neural Network with panchromatic imagery. International Journal of Remote Sensing, 2011, 32, 6149-6176.	1.3	60
166	Spatio-temporal analysis of tree height in a young cork oak plantation. International Journal of Geographical Information Science, 2011, 25, 1083-1096.	2.2	8
167	The use of MERIS Terrestrial Chlorophyll Index to study spatio-temporal variation in vegetation phenology over India. Remote Sensing of Environment, 2010, 114, 1388-1402.	4.6	118
168	Characterising the spatial pattern of phenology for the tropical vegetation of India using multi-temporal MERIS chlorophyll data. Landscape Ecology, 2010, 25, 1125-1141.	1.9	35
169	A Geostatistically Weighted <i>k</i> â€NN Classifier for Remotely Sensed Imagery. 饿"Ÿå½±åƒçš"地统è®jå Analysis, 2010, 42, 204-225.	Šæfkâ€NI 1.9	Vå^†ç±»å™°ç 34
170	Terrestrial vegetation phenology from MODIS and MERIS. , 2010, , .		3
171	Spatial Predictions of Rhodesian Human African Trypanosomiasis (Sleeping Sickness) Prevalence in Kaberamaido and Dokolo, Two Newly Affected Districts of Uganda. PLoS Neglected Tropical Diseases, 2009, 3, e563.	1.3	45
172	Issues of uncertainty in super-resolution mapping and their implications for the design of an inter-comparison study. International Journal of Remote Sensing, 2009, 30, 5293-5308.	1.3	125
173	Parameter exploration of the raster space activity bundle simulation. Journal of Geographical Systems, 2008, 10, 263-289.	1.9	0
174	Downscaling Cokriging for Super-Resolution Mapping of Continua in Remotely Sensed Images. IEEE Transactions on Geoscience and Remote Sensing, 2008, 46, 573-580.	2.7	104
175	A linearised pixel-swapping method for mapping rural linear land cover features from fine spatial resolution remotely sensed imagery. Computers and Geosciences, 2007, 33, 1261-1272.	2.0	78
176	Non-stationary variogram models for geostatistical sampling optimisation: An empirical investigation using elevation data. Computers and Geosciences, 2007, 33, 1285-1300.	2.0	49
177	Localized soft classification for superâ€resolution mapping of the shoreline. International Journal of Remote Sensing, 2006, 27, 2271-2285.	1.3	60
178	Increasing the Accuracy of Predictions of Monthly Precipitation in Great Britain Using Kriging with an External Drift. , 2006, , 243-267.		1
179	Conditional Simulation Applied to Uncertainty Assessment in DTMs. , 2006, , 269-285.		0
180	Vertical and Horizontal Spatial Variation of Geostatistical Prediction. , 2006, , 209-222.		2

11

#	Article	IF	CITATIONS
181	Pixel Unmixing at the Sub-pixel Scale Based on Land Cover Class Probabilities: Application to Urban Areas. , 2006, , 59-76.		1
182	Land Cover Map 2000 and Meta-data at the Land Parcel Level. , 2006, , 143-153.		4
183	The Effects of Uncertainty in Deposition Data on Predicting Exceedances of Acidity Critical Loads for Sensitive UK Ecosystems. , 2006, , 187-207.		1
184	Geostatistical Prediction and Simulation of the Lateral and Vertical Extent of Soil Horizons. , 2006, , 223-241.		0
185	Remote Monitoring of the Impact of ENSO-related Drought on Sabah Rainforest Using NOAA AVHRR Middle Infrared Reflectance: Exploring Emissivity Uncertainty. , 2006, , 119-142.		2
186	Super-resolution Land Cover Mapping from Remotely Sensed Imagery using a Hopfield Neural Network. , 2006, , 77-98.		7
187	Analysing Uncertainty Propagation in GIS: Why is it not that Simple?. , 2006, , 155-165.		21
188	Managing Uncertainty in a Geospatial Model of Biodiversity. , 2006, , 167-185.		0
189	Uncertainty in Remote Sensing and GIS: Fundamentals. , 2006, , 1-18.		23
190	Current Status of Uncertainty Issues in Remote Sensing and GIS. , 2006, , 287-302.		2
191	On the Ambiguity Induced by a Remote Sensor's PSF. , 2006, , 37-57.		3
192	Downscaling cokriging for image sharpening. Remote Sensing of Environment, 2006, 102, 86-98.	4.6	176
193	Superresolution mapping using a hopfield neural network with fused images. IEEE Transactions on Geoscience and Remote Sensing, 2006, 44, 736-749.	2.7	114
194	Uncertainty in Remote Sensing. , 2006, , 19-24.		13
195	Toward a Comprehensive View of Uncertainty in Remote Sensing Analysis. , 2006, , 25-35.		8
196	Deriving ground surface digital elevation models from LiDAR data with geostatistics. International Journal of Geographical Information Science, 2006, 20, 535-563.	2.2	44
197	Spatial Prediction and Surface Modeling. Geographical Analysis, 2005, 37, 113-123.	1.9	13
198	Urbanization, malaria transmission and disease burden in Africa. Nature Reviews Microbiology, 2005, 3, 81-90.	13.6	455

#	Article	IF	CITATIONS
199	Sub-pixel Target Mapping from Soft-classified, Remotely Sensed Imagery. Photogrammetric Engineering and Remote Sensing, 2005, 71, 839-846.	0.3	252
200	Superresolution Mapping Using a Hopfield Neural Network With LIDAR Data. IEEE Geoscience and Remote Sensing Letters, 2005, 2, 366-370.	1.4	83
201	The use of elevation data in flood inundation modelling: A comparison of ERS interferometric SAR and combined contour and differential GPS data. International Journal of River Basin Management, 2005, 3, 3-20.	1.5	18
202	IDENTIFICATION OF SPECIFIC TREE SPECIES IN ANCIENT SEMI-NATURAL WOODLAND FROM DIGITAL AERIAL SENSOR IMAGERY. , 2005, 15, 1233-1244.		26
203	Superâ€resolution mapping of the waterline from remotely sensed data. International Journal of Remote Sensing, 2005, 26, 5381-5392.	1.3	151
204	Spatial variation in land cover and choice of spatial resolution for remote sensing. International Journal of Remote Sensing, 2004, 25, 3687-3702.	1.3	82
205	Super-resolution land cover pattern prediction using a Hopfield neural network. Remote Sensing of Environment, 2002, 79, 1-14.	4.6	221
206	Nonâ€stationary Approaches for Mapping Terrain and Assessing Prediction Uncertainty. Transactions in GIS, 2002, 6, 17-30.	1.0	27
207	Super-resolution target identification from remotely sensed images using a Hopfield neural network. IEEE Transactions on Geoscience and Remote Sensing, 2001, 39, 781-796.	2.7	272
208	Multiple-class land-cover mapping at the sub-pixel scale using a Hopfield neural network. International Journal of Applied Earth Observation and Geoinformation, 2001, 3, 184-190.	1.4	63
209	Spatial Scale Problems and Geostatistical Solutions: A Review. Professional Geographer, 2000, 52, 607-623.	1.0	217
210	Linking remote sensing, land cover and disease. Advances in Parasitology, 2000, 47, 37-80.	1.4	56
211	Generalized linear modelling in geomorphology. , 1998, 23, 1185-1195.		60
212	Super-resolution mapping of urban scenes from IKONOS imagery using a Hopfield neural network. , 0, ,		9
213	Land cover classification from hyperspectral remotely sensed data: an investigation of spectral, spatial and noise issues. , 0, , .		1
214	Super-resolution mapping of multiple-scale land cover features using a Hopfield neural network. , 0, , .		2
215	Super-resolution mapping of the shoreline through soft classification analyses. , 0, , .		4
216	The combined effect of spatial resolution and measurement uncertainty on the accuracy of empirical atmospheric correction. , 0, , .		0

#	Article	IF	CITATIONS
217	Relating SAR image texture and backscatter to tropical forest biomass. , 0, , .		2
218	Sensitivity of a flood inundation model to spatially-distributed friction. , 0, , .		1
219	Uncertainty in Land Cover Mapping from Remotely Sensed Data Using Textural Algorithm and Artificial Neural Networks. , 0, , 99-118.		1
220	Scale in Spatial Information and Analysis. , 0, , .		42
221	Spatial Associations between COVID-19 Incidence Rates and Work Sectors: Geospatial Modeling of Infection Patterns among Migrants in Oman. Annals of the American Association of Geographers, 0, , 1-20.	1.5	3